PRAMANA
—journal of
physics

Vol. 50, No. 6,
June 1998
pp. 485–500

Ion-molecule reactions at thermal energies

S V K KUMAR
Tata Institute of Fundamental Research, Homi Bhabha Road, Colaba, Mumbai 400 005, India
E-mail: svkk@tifrc4.tifr.res.in

Abstract. Ion-molecule reactions is a generic word for reactions involving ions (both positive and negative), radicals and stable neutrals. In this presentation, use of the flowing afterglow technique to study ion-molecule reactions at thermal energies is demonstrated using the examples of positive ion-negative ion mutual neutralization of molecular nitrogen ion (N_2^+) with F^- and the reaction of atomic nitrogen with SF_n ($n = 1$ to 5) to form NF.

Keywords. Ion-molecule reactions; afterglow; radicals; mutual neutralization; fluorescence.

PACS Nos 33.50; 82.30; 82.40

1. Introduction

Ion-molecule reactions is a generic name used for the following type of reactions:

Ion-molecule (neutral) reactions

$$\begin{aligned} A^+ + B(BC) &\longrightarrow A + BC^+(B^+) + (C) \\ &\longrightarrow A^* + BC^+(B^+) + (C) \\ &\longrightarrow A + B^+(B^*) + C(C^+) \\ &\longrightarrow A + BC^{+*}(B^{+*}) + (C) \\ &\longrightarrow AB(AB^+) + C^+(C) \\ A^- + B(BC) &\longrightarrow A + BC^-(B^-) + (C) \\ &\longrightarrow A(AB) + BC(C) + e^- \\ &\longrightarrow AB^-(AB) + C(C^-). \end{aligned}$$

Neutral (radical) reactions

$$\begin{aligned} A + BC &\longrightarrow AB + C \\ A^* + BC &\longrightarrow A + BC^* \\ &\longrightarrow A + BC^+ \\ &\longrightarrow A + B + C. \end{aligned}$$

Mutual neutralization

$$\begin{aligned} A^+ + B^- &\longrightarrow A^* + B \\ A^{+*} + B^- &\longrightarrow A^{**} + B. \end{aligned}$$

There is considerable interest in the study of these reactions involving atoms, radicals and ions (both positive and negative) to understand the mechanism and dynamics [1], energy transfer, electron transfer, to test quantum mechanical theories developed for reactive and non-reactive scattering, understanding ion-molecule reactions using molecular orbital picture, etc. These reactions occur at thermal energies in various kinds of plasmas, planetary atmosphere, comets, gas lasers, combustion, gaseous dielectrics [2] and dry etch reactors [3]. With the increasing awareness of the environmental pollution that is caused by many gases that are currently in use [4] and gaseous effluents, it becomes necessary to investigate the possible reaction channels not only for the known reactive species but also involving others, at thermal energies, for practical applications. In a recent special issue of the International Journal of Mass Spectrometry and Ion Processes [5], various methods used to study neutral–neutral, ion-molecule, electron-ion recombination and ion–ion mutual neutralization reactions have been described with some recent results indicating the importance of these reactions at thermal energies.

In this presentation the use of the flowing after glow technique to produce radicals, ions, etc. and perform collision experiments at thermal energies, along with the necessary detection techniques for identifying the products and their final states will be discussed.

Ion–ion mutual neutralization of N_2^+ with F^- is chosen as an example to demonstrate the different product states (electronic and vibration) of the neutrals that are formed when the positive ion is in its ground state and excited state. The dynamics of the electron transfer in the collision will also be analysed [6]. Also, the interaction of N with SF_n ($n = 1 - 5$) will be discussed as an example of neutral–neutral collisions. The formation of the products can be understood based on both energy and symmetry considerations [7].

2. Experimental

Though there are many methods, including beam methods [8], available to study ion-molecule reactions at thermal energies the flowing afterglow method [9] is used by several groups because of its simplicity. It is well known that in an electrical discharge ions, radicals and excited species are produced mainly by electron impact and also through ion-molecule reactions and this can be exploited to produce ions or radicals of interest. These ions or radicals can easily be transported to the interaction region using fast flowing helium carrier gas so that the intensity of electrons and other unwanted species have died down, and mainly the species of interest is present. The reactant is added suitably at this point and the products formed are detected using a mass spectrometer, fluorescence or laser excitation methods. The apparatus used in our laboratory is shown in figure 1. Ions of interest are produced in a quartz discharge tube and pulled into the stainless steel observation region rapidly by a combination of a roots blower and a rotary mechanical pump with a total effective speed of 10,000 l/m. An absolute MKS Baratron is used to measure the pressure in the reaction chamber. The discharge is powered by a 2.45 GHz microwave generator and fed into an Evanston cavity enclosing the discharge tube. Helium is used as the buffer gas to help easy transportation of the ions into the observation region with little loss. A pair of grids, positioned at the exit of the discharge tube, which can be biased appropriately act as an ion shutter to stop either positive or negative ions. The grids are so biased that ions enter the observation region at earth potential and no external field gradients are present.

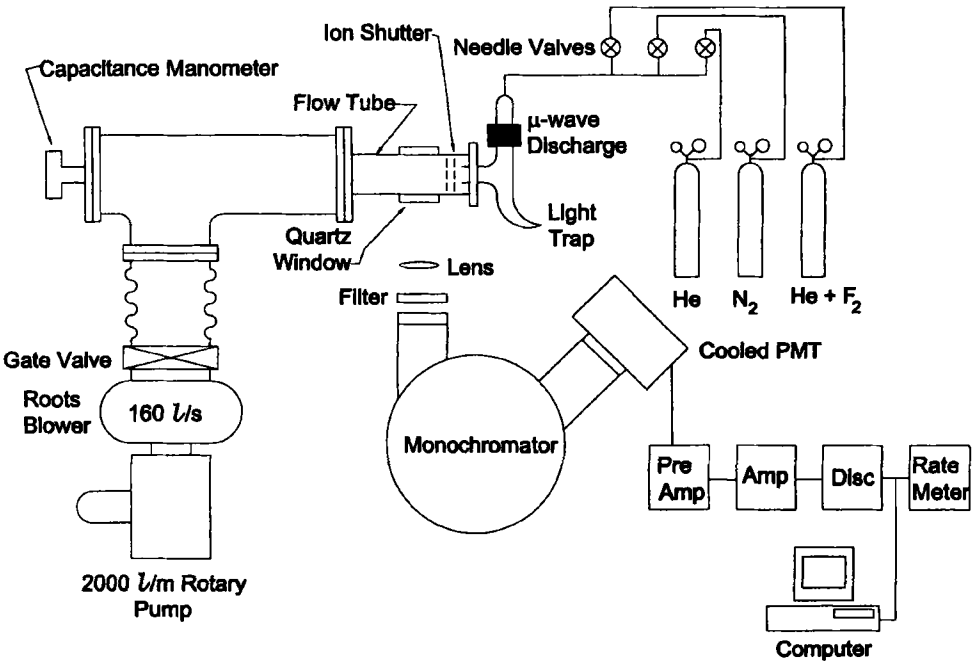

Figure 1. Schematic view of the flow reactor set up.

Fluorescence from the reaction products is monitored through a quartz window and focused on to the entrance slit of a 0.2 m Seya-Namioka monochromator and detected by a cooled photomultiplier (Hamamatsu R376) operating in the photon counting mode. A cutoff filter with 96% transmission efficiency above 400 nm is utilized to suppress the interference of second order lines from the UV region. A PC based multi-channel scaler is employed for data acquisition. A tungsten–halogen lamp is used to determine the response of the detection system as a function of the wavelength. All the data presented here have been corrected for the system response. The fluorescence from the interaction region showed a decrease in the intensity when the grids were biased to stop either the positive or the negative ions. The contribution to the fluorescence signal from the reaction of charge particles is elucidated by subtracting the spectrum recorded with the bias on (no contribution from the interaction of charged particles but only from neutral reactions and other sources) from the spectrum when both the grids were maintained at earth potential (signal from the reaction involving charged particles and from neutral reactions and other sources).

99.99% pure nitrogen, 99.995% pure helium, >99.9% pure sulphur hexafluoride, and laser grade fluorine in 99.998% pure helium mixture were used without further purification for the experiments.

The setup was suitably modified to work with radicals. Atomic nitrogen was produced by a DC discharge 60 cm upstream from the interaction zone and a larger diameter tube (40 mm) was used to transport the radicals to the interaction zone. This was necessary to avoid the presence of higher excited states of N_2 other than the long lived $A\ ^3\Sigma_u^+$. Small

amounts of SF_6 were discharged (DC) separately along with helium, which was used as the buffer gas, to produce SF_n ($n = 1$ to 5) radicals which could be transported to the interaction region with very little loss. Atomic nitrogen and SF_n ($n = 1$ to 5) radicals were mixed in the main flow tube and the observation region was located 20 mm downstream of the mixing zone.

Spectrum in the range 200 to 800 nm was recorded for pure nitrogen discharge at several pressures and currents and monochromator resolution to monitor the presence of any impurities. SF_6 was then added through the second discharge tube without the discharge being on and, with and without helium buffer to check for any reactions and/or quenching of the N_2 spectrum. Spectrum was recorded to look for metastable fluorescence from SF_6 discharge products separately with nitrogen flow completely shut off. Nitrogen and SF_6 were mixed together prior to the discharge and an afterglow spectrum was recorded to ascertain all the lines in the spectrum. This procedure helped to identify clearly that the product NF was produced only due to the reaction of atomic nitrogen with the discharge products of SF_6.

3. Results and discussion

3.1 *Ion–ion mutual neutralization*

Background counts in the afterglow region of the helium discharge were below the detection limit of the photomultiplier tube between 200–800 nm for the pressure range 0.06–0.07 Torr and 10 to 40 W of microwave power. The addition of 0.0101 Torr of nitrogen to the discharge produces a weak afterglow spectrum of N_2 ($B\,^3\Pi_g \rightarrow A\,^3\Sigma_u^+$) indicating the population of lower vibrational levels of the B-state. The grids were biased to stop positive ions and electrons one at a time to check the possibility of electron-ion recombination which could produce either N_2 or N in an excited state. Under the present experimental conditions no discernible change in the intensity of N_2^* or additional emission lines from N^* could be observed. The electrons most likely diffuse towards the walls by the time the ions travel from the discharge to the observation region [10, 11] which gives the electron-ion recombination reaction little probability to be detectable.

A large increase in the intensity of the N_2 ($B\,^3\Pi_g \rightarrow A\,^3\Sigma_u^+$) fluorescence is observed when small quantities of F_2 is added to the discharge. It may be mentioned that extreme care must be taken in handling fluorine. The addition of small quantities of fluorine to the helium buffer was found to quench the discharge completely. It was necessary to use 5% fluorine in helium mixture and non-corrosive passivated gas lines to ensure that fluorine was not contaminated during injection into the discharge. 0.003–0.0045 Torr of F_2 in helium mixture was added to the discharge to produce an ion–ion plasma. The emission from the high vibrational levels of the B-state shows a systematic decrease by an equal amount in the intensity when the grids are biased either to stop positive ions or negative ions. This indicates that the change in intensity most probably arises due to the interaction between positively and negatively charged particles. Under the conditions of the experiment, it can be assumed with reasonable confidence that an ion–ion plasma exists in the interaction region [10, 11]. The helium buffer pressure was varied from 0.04 to 0.09 Torr to check for any influence of the buffer gas on the observed vibrational

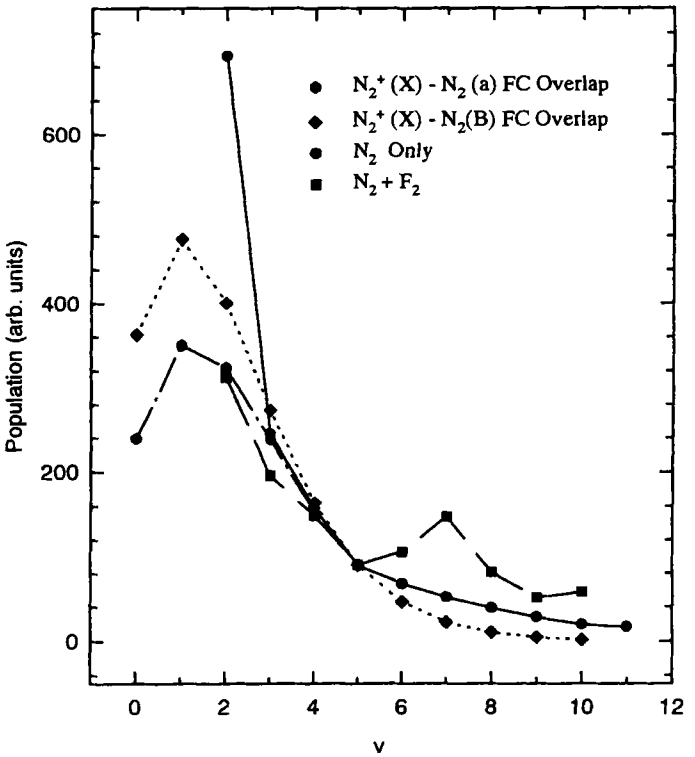

Figure 2. Comparison of the population of the $N_2(B)$ vibrational levels resulting from neutral recombination ($N + N \rightarrow N_2(B)$) in a N_2 + He afterglow, theoretical distribution calculated using the Franck–Condon overlap as described in the text, and experimentally observed distributions when F_2 is added to the discharge.

population distribution of $N_2(B)$. No measurable change could be noticed in the intensity of the spectral lines populating the $N_2(B)$ via the positive ion-negative ion neutralization (PININ) processes.

The population of the vibrational levels of the product $N_2(B)$ state formed by the positive ion–negative ion neutralization reaction

$$N_2^+ + \text{negative ion} \rightarrow N_2^* + \text{neutral} \tag{1}$$

is calculated by appropriately weighting the intensity of each line by its Franck–Condon factor [12]. The relative population distribution of the vibrational levels derived from the above experiments are normalized at $v' = 5$ and presented in figure 2.

The results depicted in figure 2 indicate that the population of the $N_2(B)$ vibrational levels, formed mainly by atomic recombination in the afterglow, shows a steady decrease in the intensity from $v' = 2$–11. The population distribution shows a similar trend from $v' = 2$–5 for the product state formed by positive ion–negative ion neutralization from nitrogen with F_2 discharge. However, beyond $v' = 5$ there is an increase in the intensity peaking at $v' = 7$ before the intensity drops down again, indicating a second preference

for higher vibrational levels. These are probably the first observations of preferences for higher vibrational states of the product in a PININ reaction.

In the PININ process the electron from the negative ion is expected to hop to the positive ion when the incoming ionic potential energy surface goes through an avoided curve crossing with the outgoing repulsive covalent potential surface corresponding to the product state of the two neutrals [13, 14]. The electronic configuration of $N_2^+(X\,^2\Sigma_g^+)$ is $1\sigma_g^2\ 1\sigma_u^2\ 2\sigma_g^2\ 2\sigma_u^2\ 1\pi_u^4\ 3\sigma_g^1$ and that of $F^-(^1S)$ is $1s^2\ 2s^2\ 2p^5$. Simplified symmetry

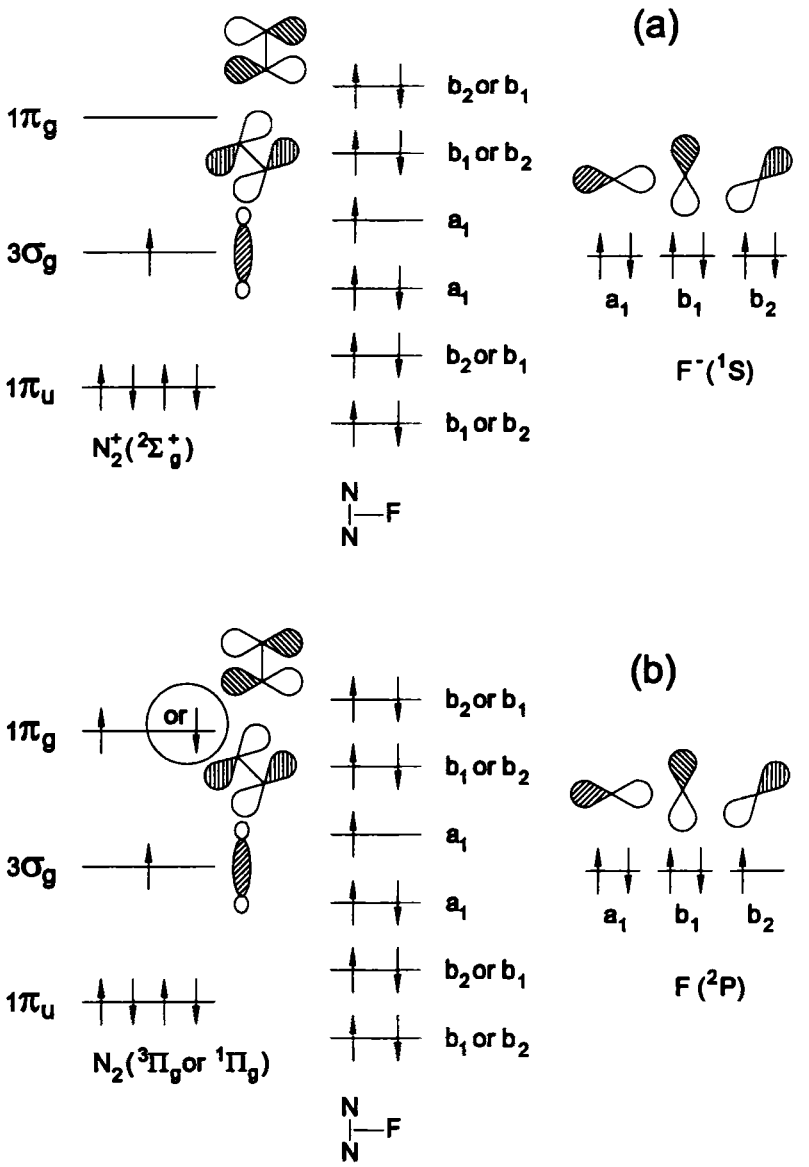

Figure 3. (*Continued*).

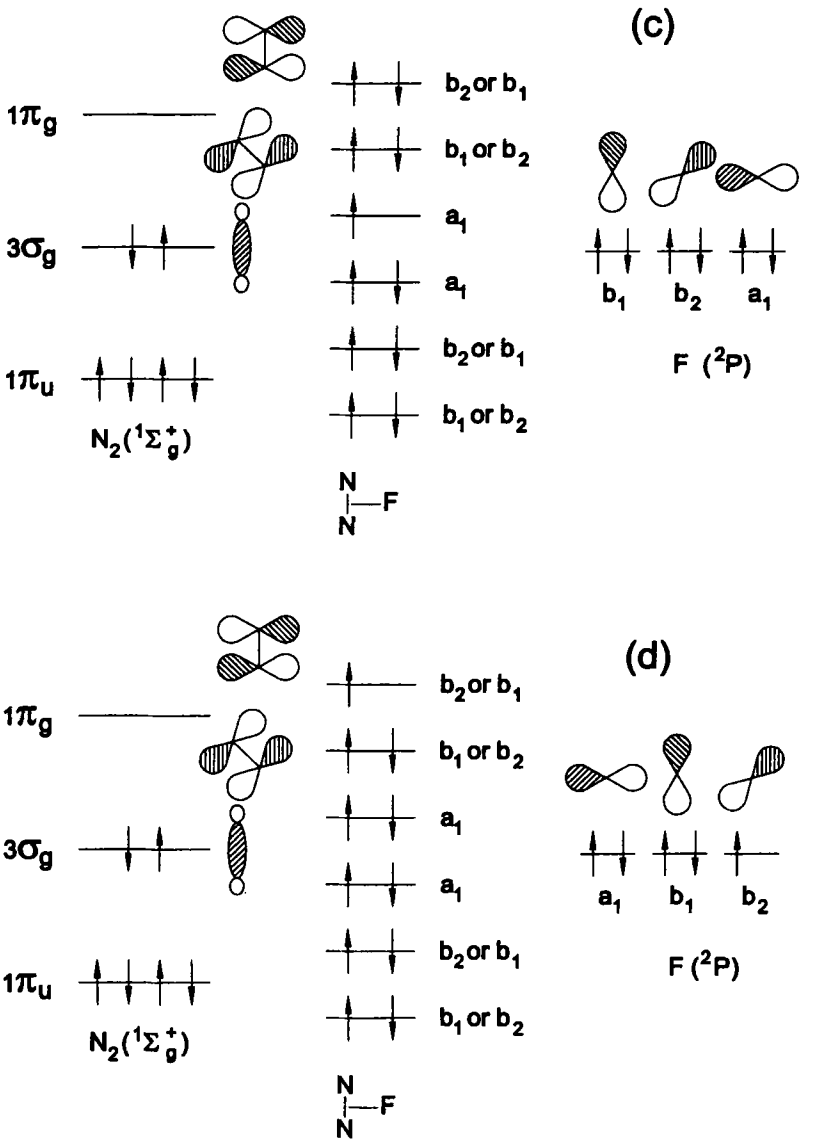

Figure 3. Symmetry adapted linear combination of orbitals for (**a**) (^2A) $N_2^+ - F^-$ incoming channel correlating with (**b**) (^2A) N_2 ($^3\Pi_g$ or $^1\Pi_g$)–F(^2P) outgoing channels; (**c**) the (^2A) N_2 ($^1\Sigma_g^+$)–F(^2P) outgoing channel; and (**d**) not correlating with the (^2B) N_2 ($^1\Sigma_g^+$)–F(^2P) outgoing channel.

considerations have been used to derive orbital energy diagrams shown in figure 3 for the intermediate states possible in the PININ process.

For the neutralization reaction, the $2p_x$, $2p_y$ or $2p_z$ electron from F^- must fill the first virtual $1\pi_g$ orbital of N_2 to form either $N_2(B\ ^3\Pi_g)$ or $N_2(a\ ^1\Pi_g)$ states. Only one of the p orbitals of F^- would interact with the $3\sigma_g$ orbital of N_2^+ to give two a_1 orbitals, one

containing the unpaired electron, giving a ^2A state of the N_2–F intermediate. Considerations of the orbital diagrams suggest that the interaction between $F(^2P)$ and $N_2(B\,^3\Pi_g$ or $a\,^1\Pi_g)$ may give rise to the same state of the N_2 – F intermediate (^2A). This indicates that N_2 – F can dissociate to give N_2 either in an excited $^3\Pi_g$ (or $^1\Pi_g$) or in the ground state $^1\Sigma_g^+$ and $F(^2P)$. The interaction between $N_2(X\,^1\Sigma_g^+)$ and $F(^2P)$ gives rise to a ^2B state of the intermediate which, however, is not correlated with the N_2–$F(^2A)$ formed from $N_2^+(X\,^2\Sigma_g^+)$ and $F^-(^1S)$. This makes the formation of $N_2(^1\Sigma_g^+)$ from $N_2^+ + F^-$ a low probability PININ process. Rearrangement of the electrons is necessary for the formation of $N_2(C\,^3\Pi_u)$ $(1\sigma_g^2\ 1\sigma_u^2\ 2\sigma_g^2\ 2\sigma_u^1\ 1\pi_u^4\ 3\sigma_g^2\ 1\pi_g^1)$ by mutual neutralization. Therefore, this channel is likely to have a low cross section and has not been detected during the course of these experiments. N_2^+ ions are formed in the discharge mainly by electron impact and to a certain extent by Penning ionization from helium metastables. Penning ionization of N_2 by He^* produces N_2^+ both in the ground state as well as excited states [15]. As no fluorescence from the excited N_2^+ is detectable in the observation region it can be safely assumed that only N_2^+ ions in their ground state interact with the negative ions.

As the PININ process occurs in most cases at large internuclear separation between the positive and negative ions the Born–Oppenheimer approximation is valid [16–18]. Therefore the population of the final levels of the product state is expected to be determined by the Franck–Condon overlap between the potential energy surface corresponding to the electronic state of the positive ion and that of the neutral product. The Franck–Condon overlap for the transitions from $N_2^+(X\,^2\Sigma_g^+)$ to $N_2(B\,^3\Pi_g)$ and $N_2(a\,^1\Pi_g)$ were calculated using the code 'level' (ver. 5.1) [19] assuming that the vibrational distribution of the $N_2^+(X\,^2\Sigma_g^+)$ state is governed by the Franck–Condon factors for ionization from the ground state of the N_2 molecule. This appears to be a reasonably valid approximation as N_2^+ ions are produced mainly by electron impact in the discharge and to a certain extent by Penning ionization. In both cases [19, 20] the Franck–Condon principle is valid for the ionization of N_2. The Franck–Condon overlap calculations, however, predict that the maximum population for both $N_2(B)$ and $N_2(a)$ is at $v' = 1$ and then smoothly decreases as a function of v' (see figure 2). The $N_2(a \rightarrow X)$ fluorescence could not be monitored as it is in the vacuum ultraviolet range. The relative population distribution, as determined experimentally, appears to follow the Franck–Condon distribution for the $B\,^3\Pi_g$ state from $v' = 2$–5 but shows an additional preference for higher vibrational levels from $v' = 6$–9 with a maximum at $v' = 7$ for the PININ reaction with F^- and F_2^-. Such preferences are known to exist in energy transfer to N_2 from $Kr(^3P_2)$ [21] due to avoided curve crossings.

Using similar empirical considerations [21] to achieve a quantitative characterization of the surfaces in the crossing region for the N_2–F system, as needed for the accurate treatment of the dynamics, the entrance channel is modeled as an ionic surface by an extension of the Rittner model for alkali halides [22–25], accounting for specific electrostatic properties induced by F^- [26] and N_2^+ [27, 28] and assuming that N_2^+ is in its ground ($v = 0$) vibrational level. The exit channel is represented as a vibronic manifold of surfaces [21, 29, 30].

The two limiting geometries of approach, parallel and perpendicular, are explicitly considered as arising from the anisotropy of the $N_2^+(^2\Sigma_g^+)$ ion and of the nitrogen molecule in the $^3\Pi_g$ state. The latter is assumed in the vibrational modes from zero to ten

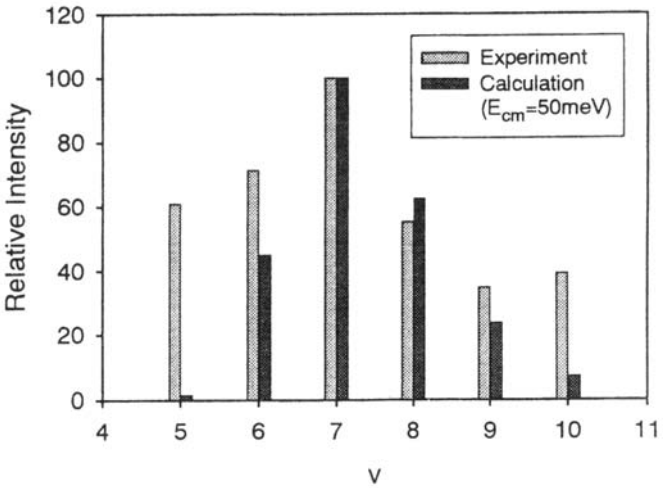

Figure 4. Comparison of the relative cross sections, for the $N_2^+ + F^-$ reaction, as a function of the vibrational levels v of the product $N_2(B)$, at a collision energy of 50 meV. The calculated cross sections for the various exit channels are normalized to $v = 7$ and compared with the experimental results.

included, to cover the range experimentally relevant. As will be seen, in view of the relatively large distances where the corresponding crossings occur, the molecular anisotropy will manifest itself as a minor effect on the dynamics. Along the same line, we can also justify the neglect of electronic anisotropy of the fluorine atom in the exit channel, for which a single electronic surface is considered.

Figure 4 shows a comparison between the distributions calculated for the reaction $\rightarrow N_2(B) + F$ at the most probable collision energy, which is estimated to be ~ 50 meV, and the experimentally measured distributions. Calculations were carried out at three different energies 25, 50 and 75 meV. It was found that the vibrational population distribution of $N_2(B)$ varied very little with the collision energy in this range.

The similarity of calculated distributions at the three energies shown, proves that averaging over thermal distribution does not alter the over-all picture. It is observed that overall difference between the calculated and observed distributions is reasonably good. The difference between the calculated and the experimental distributions are not surprising, considering that possibility of higher vibrational levels being populated and other possible alternative processes occurring in the discharges (see the extensive discussion in ref. [6]) have been neglected.

It can be inferred that, such a propensity appears as a balance of two trends: (i) according to Franck–Condon factors, the level $v = 1$ should be favored and the propensity should decrease for high v; (ii) on the contrary, as far as the role of dynamics is concerned, since crossings of higher v levels occur at larger distances, the propensity should be in favor of the high v and decrease as a function of the vibrational quantum number of the outgoing channel. This results in the peaking of the population of the vibrational levels of $N_2(B)$ product at $v = 7$, formed by the $N_2^+ + F^-$ PININ reaction.

3.2 *Radical–radical reactions*

To study the interaction of N with SF_n radicals, experiments were conducted in the modified apparatus so that little ions reached the interaction region. Observations were done at total pressures of 0.06 to 0.1 Torr and 0.35 to 0.5 Torr for discharge currents of 15 mA each, fed by DC power supplies working in the constant current mode. Partial pressures of N_2 and $He + SF_6$ were kept equal and the SF_6 content was 5% of the total pressure. The interaction region was scanned for the fluorescence from metastable $N_2(A)$ state as well as from reaction products. It was noticed that for low pressure discharges the characteristic 530 nm radiation emanating from the $NF(b\ ^1\Sigma^+ \rightarrow X\ ^3\Sigma^-)$ transition was not observed, although fairly intense $N_2(A\ ^3\Sigma_u^+ \rightarrow X\ ^1\Sigma_g^+)$ bands were recorded. This strongly suggested that any reaction of $N_2(A)$ with SF_n ($n = 1$ to 5) or F did not result in NF(b). The 530 nm $NF(b \rightarrow X)$ radiation was observed when the discharge products of N_2 and SF_6 were mixed at total pressures more than 0.35 Torr. Both the discharges were switched off one at a time to make sure that the observed product spectrum was solely due to the interaction of the products produced by the two discharges. SF_n (where $n \leq 5$) and F, are known to be formed in sufficient numbers in SF_6 discharges.

$He + SF_6$ discharge products cannot react with N_2 to produce NF as the dissociation energy of N_2 is too high (9.76 eV). Also, experiments conducted at low pressures when $N_2(B)$ was present in the interaction region did not reveal the presence of NF(b). $N_2(A)$ cannot interact with atomic fluorine to produce NF as the reaction is expected to be endothermic by at least 0.8 eV, if the heat of formation (ΔH_f) of NF is taken to be 2.384 eV as recommended by Wategaonkar *et al* [31].

The NF(X) product could be probed by the excitation transfer process [32]

$$N_2(A) + NF(X) \rightarrow N_2(X) + NF(b). \tag{2}$$

It has been mentioned earlier in this presentation that $N_2(A)$ has been detected in sufficiently large intensities in the interaction zone at lower, as well as, higher pressures. At low pressures, probability for the two-step process, i.e. the formation of NF(X) and excitation to NF(b) by energy transfer from $N_2(A)$ is likely to be small and therefore could not be detected. At higher pressures, the collision probability increases enabling the detection of NF via the energy transfer process.

Formation of NF through

$$N + F + M \longrightarrow NF + M, \tag{3}$$

where M is a third body (or wall), is likely to have a low cross section. For instance, no $NF(b \rightarrow X)$ fluorescence was observed from the interaction region even though atomic fluorine was present [7]. Atomic $N(^2D \rightarrow {}^4S)$ radiation was not observed indicating its absence in the reaction region because of the distance between the discharge and the observation points. Interaction of the excited states of atomic nitrogen with the discharge products of SF_6 to produce NF may not be considered under the experimental conditions. Other processes like

$$N^+(^3P) + F^-(^1S) \rightarrow NF(^1\Sigma^+) \quad \text{or} \quad NF(^3\Sigma^-) \tag{4}$$

need not be considered as well, as the Wigner spin rule does not allow the mutual recombination reaction. Also, because of various crossings with repulsive potential energy curves it has a tendency to dissociate rather than form a bound NF state.

SF_n ($n = 1$ to 5) and F are produced by electron impact dissociation, ion-molecule reactions and neutral–neutral reactions in corona [4, 33], RF [34–36] and other type of SF_6 discharges. SF_4, SF_2 and F have been detected outside the discharge region in corona (pressures of 1 bar and above) [4, 33], RF (a few Torr) [36] and DC [37] discharges in pure SF_6 and mixtures with O_2, N_2 and Ne because of their relatively higher stability compared to SF_5 and SF_3. By using a dilute mixture of SF_6 in helium, it helps in not only reducing the neutral–neutral reactions in which SF_5 and SF_3 are destroyed but also in quickly transporting them to the interaction region so that the reactions which occur in the discharge zone can be studied easily with less interference from other competing reactions. The following reactions of atomic nitrogen with the SF_6 discharge products are considered based on the heats of formation given by Herron [38], symmetry and structure of SF_n ($n = 1$ to 5) by Ziegler and Gustev [39] and for SF_6 by Herzberg [40].

$$N(^4S_{3/2}) + SF(^2\Pi) \rightarrow NF(X\,^3\Sigma^-) + S(^3P_2) - 0.229\,\text{eV}, \tag{5}$$

$$N(^4S_{3/2}) + SF_2(^1A_1) \rightarrow NF(X\,^3\Sigma^-) + SF(^2\Pi) - 0.839\,\text{eV}, \tag{6}$$

$$N(^4S_{3/2}) + SF_3(^2B_1) \rightarrow NF(X\,^3\Sigma^-) + SF_2(^1A_1) + 0.518\,\text{eV}, \tag{7}$$

$$N(^4S_{3/2}) + SF_4(^1A_1) \rightarrow NF(X\,^3\Sigma^-) + SF_3(^2B_1) - 0.344\,\text{eV}, \tag{8}$$

$$N(^4S_{3/2}) + SF_5(^2A_1) \rightarrow NF(X\,^3\Sigma^-) + SF_4(^1A_1) + 0.958\,\text{eV}, \tag{9}$$

$$N(^4S_{3/2}) + SF_6(^1A_{1g}) \rightarrow NF(X\,^3\Sigma^-) + SF_5(^2A_1) - 0.685\,\text{eV}. \tag{10}$$

Energetics allow reactions (7) and (9) to proceed and not (5), (6), (8) and (10).

Production of NF by the interaction of $N_2(B\,^3\Pi_g,\ v' = 0)$ with SF_n ($n = 1$ to 6) is not possible as the reactions are endothermic at room temperature. However, the following reactions involving vibrationally excited $N_2(B)$

$$N_2(B, v' \geq 10) + SF_3 \longrightarrow NF(X) + SF_2 + N, \tag{11}$$

$$N_2(B, v' \geq 7) + SF_5 \longrightarrow NF(X) + SF_4 + N, \tag{12}$$

are energetically allowed. It has been observed from our low pressure experiments that though SF_6 does not quench the $N_2(B)$ state, but the dissociation products of SF_6 do quench the $N_2(B)$. If NF could be formed through reactions (11) and (12) then the intensity of the observed $N_2(B \rightarrow A)$ lines corresponding to $v' \geq 7$ should be much lower than for $v' \leq 6$, as the NF formation channel opens up. This is however not the case and the quenching cross section is the same for all $v' = 2$ to 11. Hence, the reactions (11) and (12) appear to have very small cross section values.

S_2F_{10}, which is formed by the combination of two SF_5 molecules [41], cannot react with molecular nitrogen, its excited states or atomic nitrogen to produce NF as they are not allowed solely on the basis of energy considerations. Small amounts of water vapor or addition of oxygen to SF_6 in discharges produce SOF_4, SOF_2 and SOF [4, 7, 36, 37, 42, 43]. The change in the $NF(b \rightarrow X)$ fluorescence was not perceptible when traces of oxygen were added separately to N_2 and SF_6 discharges. Interaction of atomic nitrogen with these species favors the formation of NO while the NF channel is ruled out as it is endothermic. HF which is produced in the discharge due to water vapor impurity cannot react with atomic nitrogen to form NF because of the same reason.

Thus the most likely channels producing NF are reactions 7 and 9. Of these, the latter is more likely to be dominant over the former for several reasons:

(i) The rate constant for the production of SF_5 by electron impact dissociation and dissociative ionization is more compared to that of SF_3 [4, 5, 41]. In addition, SF_5 is

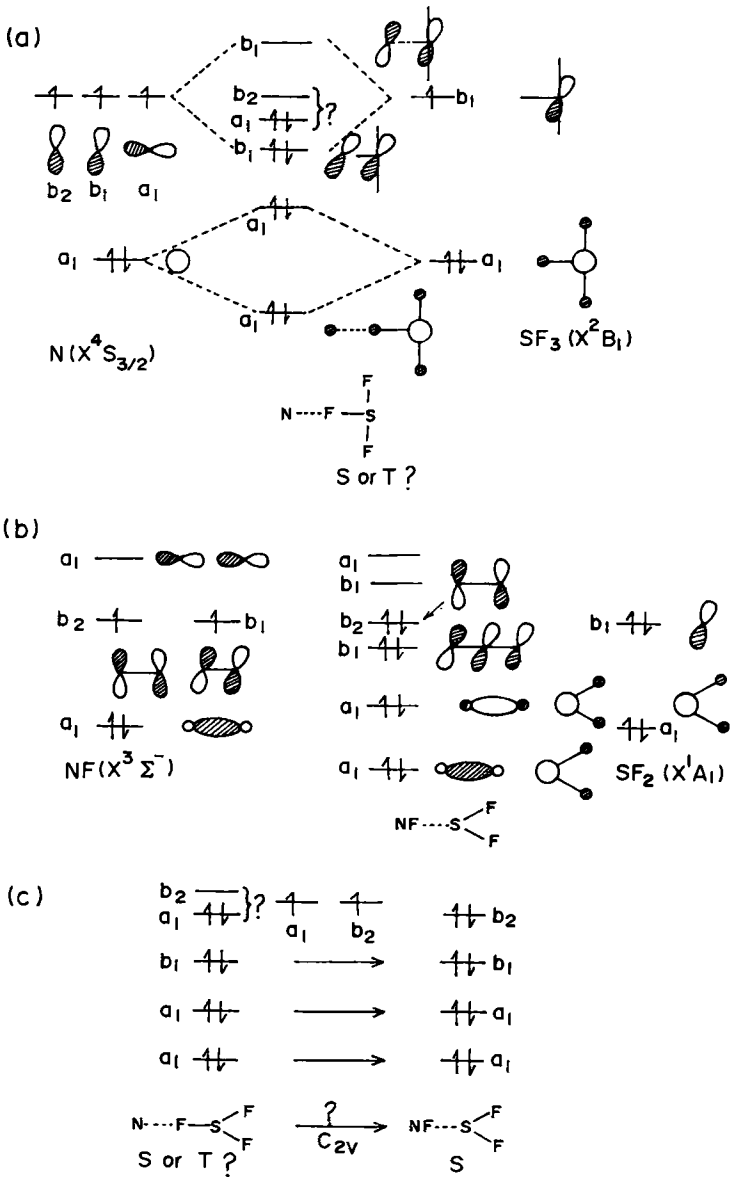

Figure 5. Symmetry adapted linear combination of orbitals for (**a**) $N\cdots FSF_2$ and (**b**) $NF\cdots SF_2$ in C_{2v} geometry; (**c**) correlation (or lack thereof) of the orbitals between ground states of reactants and products.

likely to be produced outside the discharge region by ion-molecule reactions like

$$SF_4^+ + SF_6 \rightarrow SF_5 + SF_5^+. \quad (13)$$

(ii) The exoergicity of reaction (9) is larger than that of reaction (7). This means that there are more product states available in the case of the former than in the latter. Also, the product SF_4 would have inherently larger density of states than SF_2. Therefore, statistically [44] reaction (9) would be more preferred.

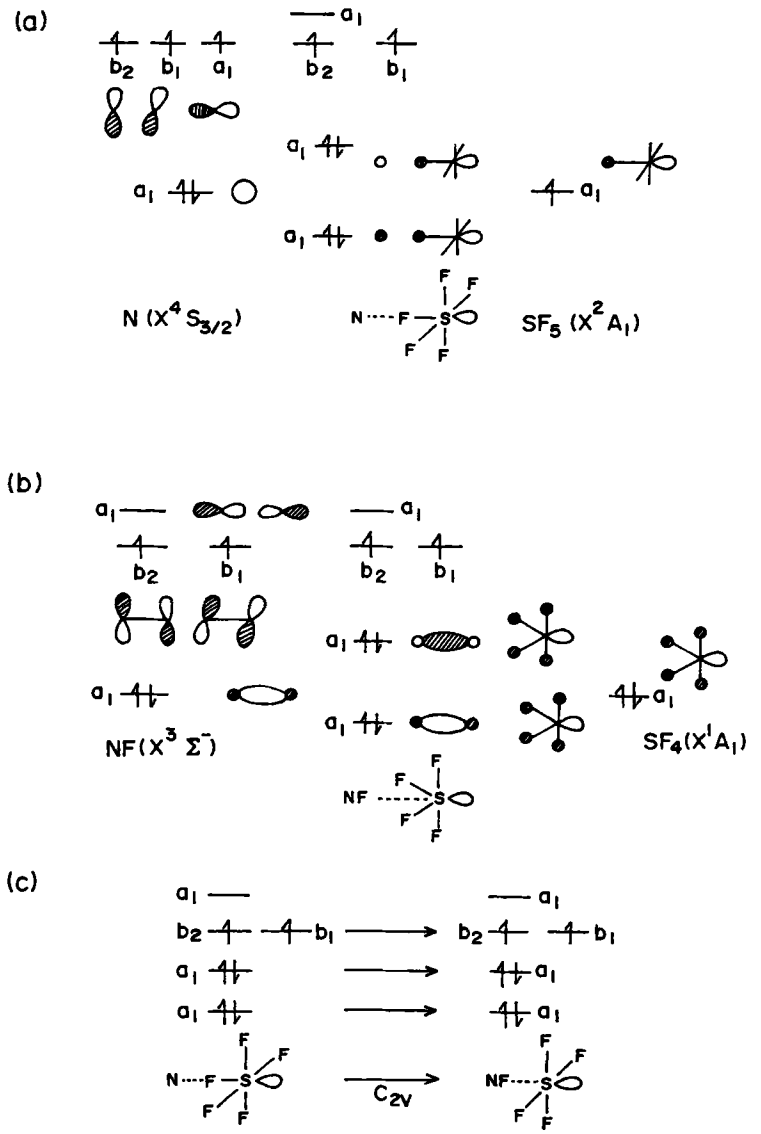

Figure 6. Symmetry adapted linear combination of orbitals for (**a**) $N\cdots FSF_4$ and (**b**) $NF\cdots SF_4$ in C_{2v} geometry; (**c**) orbital correlation between ground states of reactants and products.

(iii) A closer examination of the orbital correlation diagram suggests that reaction (7) may not be allowed by symmetry considerations [45].

Since reliable electronic structure calculations for the systems under consideration are quite involved, we have restricted ourselves to a preliminary investigation of the symmetry elements concerned. Using the orbital energy diagrams given by Ziegler and Gustev [39] for the valence electrons of SF_n ($n = 1$ to 5), we have constructed the schematic orbital energy diagrams for NSF_3 and NSF_5 systems in C_{2v} geometry in figures 5 and 6 respectively.

In figure 5(a) we show the linear combination of orbitals of N and SF_3 in C_{2v} geometry. Only one of the three p orbitals of N would interact with the b_1 orbital of SF_3. The b_2 and a_1 are likely to remain unaffected and thus degenerate, except for a possible interaction of a_1 with the lower lying a_1 orbital. Similarly, in the case of NF–SF_2 interaction shown in figure 5(b), the b_1 orbitals of NF and SF_2 would combine readily while the b_2 and a_1 would remain unaffected. This would imply that NF$\cdots$$SF_2$ would be a singlet. In the case of N + SF_3, depending upon the a_1 and b_2 orbitals being degenerate or not, the lowest electronic state would be a triplet or a singlet respectively. As shown in figure 5(c), if the ground state of the reactants is a triplet it would *not* correlate with the ground state of the products. If the former is a singlet with a_1 being lower in energy than b_2, once again the ground state of the reactants and that of the products would not correlate. Only if the b_2 orbital is lower in energy than the a_1 will the ground state of NSF_3 be correlated with the ground state of $NFSF_2$.

Using similar arguments, one can show that the highest occupied molecular orbitals are most likely a degenerate pair of b_1 and b_2 orbitals for N$\cdots$$FSF_4$ as well as NF$\cdots$$SF_4$ as illustrated in figures 6(a) and (b) respectively. This would mean that we are dealing with a triplet state for the reactants and a triplet state for the products and that both of them correlate with each other as illustrated in figure 6(c).

Though the above arguments are tentative, in the sense that, concerted reactions in C_{2v} geometries are assumed and have also relied on the qualitative MO picture, it is reasonable to consider that the formation of NF through N + SF_5, is the most likely dominant channel.

4. Conclusion

The population of the higher vibrational levels of N_2 produced by PININ, which seems to be different from that predicted by the Franck–Condon overlap. This can be attributed to the avoided curve crossing of the $N_2^+ - F^-$ potential energy surface with the $N_2(B)$–F hypersurface and the dynamics. To the best of our knowledge, this is the first observation of such a behavior in a mutual neutralization reaction. More experiments as well as theoretical calculations are necessary to completely understand the interaction of the negative ions with molecular ions and the dynamics of electron transfer.

Energy transfer from $N_2(A)$ has been utilized successfully to detect the ground state reaction product NF arising from $N_2 + SF_6$ discharges. It is argued that the most likely channel for the production of NF is the reaction between N and SF_5.

Acknowledgements

The author is thankful to S Mazumdar, N Sathyamurthy (Indian Institute of Technology, Kanpur), V Aquilanti (University of Perugia, Italy) and late S K Mitra for their contribution to these results.

References

[1] S J Watgaonkar and D W Setser, *J. Chem. Phys.* **90**, 6223 (1989)
[2] J M Meek and J D Craggs, *Electrical Breakdown of Gases* (Wiley, Chichester, 1978)
[3] R d'Agostino and D L Flamm, *J. Appl. Phys.* **52**, 162 (1981)
[4] R J Van Brunt and J T Herron, *IEEE Trans. Elec. Insul.* **25**, 75 (1990)
[5] *Int. J. Mass Spectrom. Ion Process.* **149/150**, (1995)
[6] S V K Kumar, S Mazumdar and S K Mitra, *Chem. Phys. Lett.* **237**, 448 (1995)
V Aquilanti, R Condori, S V K Kumar and F Pirani, *Chem. Phys. Lett.* **237**, 456 (1995)
[7] S V K Kumar, N Satyamurthy, S Manogaran and S K Mitra, *Chem. Phys. Lett.* **222**, 465 (1994)
[8] A Merz, M-W Ruf, H Hotop, M Movre and W Meyer, *J. Phys.* **B27**, 4973 (1994)
[9] T M Miller, J F Friedman, A E Stevens Miller and J F Paulson, *Int. J. Mass Spectrom. Ion Process.* **149/150**, 111 (1995)
T Gougousi, R Johnsen and M F Golde, *Int. J. Mass Spectrom. Ion Process.* **149/150**, 131 (1995)
[10] D Smith, N G Adams and E Alge, *J. Phys.* **B17**, 461 (1984)
[11] D Smith and P Španěl, *Adv. Atom. Mol. Opt. Phys.* **32**, 307 (1994)
[12] A Lofthus and H Krupenie, *J. Phys. Chem. Ref. Data* **6**, 113 (1977)
[13] D R Bates, *Adv. At. Mol. Phys.* **20**, 1 (1985)
[14] M R Flannery, *Adv. At. Mol. Opt. Phys.* **32**, 117 (1994)
[15] A J Yencha, in *Electron Spectroscopy: Theory, Techniques and Applications* edited by C R Brundle and A D Baker (Academic, London, 1984) vol. 5, p. 197
[16] J Weiner, W B Peatman and R S Berry, *Phys. Rev.* **A4**, 1824 (1971)
[17] J T Mosely, R E Olson and J R Peterson, in *Case Studies in Atomic Physics* edited by M R C McDowell and E W McDaniel (North Holland, Amsterdam, 1975) vol. 5, p. 1
[18] L Mémdez, I L Cooper, A S Dickinson, O Mó and A Riera, *J. Phys.* **B23**, 2797 (1990)
[19] R J LeRoy, Rep. CP-330R (Univ. Waterloo, 1992)
[20] T D Märk in *Electron Impact Ionization* edited by T D Märk and G H Dunn (Springer, Wien, 1985) Ch. 5, p. 137
[21] V Aquilanti, R Candori, F Pirani, T Krümpelmann and Ch Ottinger, *Chem. Phys.* **142**, 47 (1990)
[22] E S Rittner, *J. Chem. Phys.* **19**, 1030 (1951)
[23] Y P Varshni and R C Shukla, *J. Mol. Spectrosc.* **16**, 63 (1965)
[24] S H Patil, *J. Chem. Phys.* **86**, 313 (1987)
[25] S H Patil, *J. Chem. Phys.* **89**, 6357 (1988)
[26] A A S Sangachin and J Shanker, *J. Chem. Phys.* **90**, 1061 (1989)
[27] E F McCormack, S T Pratt, J L Dehmer and P M Dehmer, *Phys. Rev.* **A44**, 3007 (1991)
[28] K P Huber, Ch Jungen, K Yoshino, K Ito and G Stark, *J. Chem. Phys.* **100**, 7957 (1994)
[29] E Bauer, E R Fisher and F R Gilmore, *J. Chem. Phys.* **51**, 4173 (1969)
[30] V Aquilanti, R Candori, F Pirani and Ch Ottinger, *Chem. Phys.* **187**, 171 (1995)
[31] S J Wategaonkar, K Y Du and D W Setser, *Chem. Phys. Lett.* **189**, 586 (1992)
[32] K Y Du and D W Setser, *J. Phys. Chem.* **96**, 2553 (1992)
[33] I Sauers and G Harman, *J. Phys.* **D25**, 761 (1992)
[34] A Picard, G Turban and B Grolleau, *J. Phys.* **D19**, 27 (1986)
[35] L E Kline, *IEEE Trans. Plasma Sci.* **14**, 145 (1986)
[36] N Mutsukura and G Turban, *Plasma Chem. Plasma Process.* **10**, 27 (1990)

[37] W W Brandt and T Honda, *J. Appl. Phys.* **60**, 1595 (1986)
[38] J T Herron, *J. Phys. Chem. Ref. Data* **16**, 1 (1987)
[39] T Ziegler and G L Gutsev, *J. Chem. Phys.* **96**, 7623 (1992)
[40] G Herzberg, *Electronic Spectra and Electronic Structure of Polyatomic Molecules* (Van Nostrand, Princeton, 1966)
[41] J T Herron, *Int. J. Chem. Kinetics* **19**, 129 (1987)
[42] R J Van Brunt and M C Siddagangappa, *Plasma Chem. Plasma Process.* **8**, 207 (1988)
[43] I Sauers and G Harman, *J. Phys.* **D25**, 774 (1992)
[44] For example, see J C Light in: *Atom-Molecule Collision Theory* edited by R B Bernstein (Plenum Press, New York, 1979) ch. 19
[45] R B Woodward and R Hoffmann, *The Conservation of Orbital Symmetry* (Verlag Chemie, 1971)